Journal of Template

Vol. 00, No. 0, 0000

Defect imaging with guided waves propagating in a long range*

Takahiro Hayashi** Masahiro Nagao** and Morimasa Murase**
**Nagoya Institute of Technology,
Gokiso Showa Nagoya, 466-8555, Japan
E-mail: hayashi@nitech.ac.jp

Abstract

Pipe inspection with guided waves is expected to provide an efficient screening technique that will enable the inspection of lengths of pipe of up to a few dozen meters. In contrast with conventional inspection equipment widely used in practical inspection that employ easy-to-use axisymmetric modes, the present authors have developed a defect imaging technique that uses non-axisymmetric modes. In a previous paper, defect images were only available over a short range of 1.2 meters from the transducers. Therefore, in the present study, the effects of long propagation on defect images are discussed. Long-range imaging was performed experimentally using source signals and their multiple reflections between both edges of a four-meter-long pipe, rather than the reflected waves from defects. In the experimental investigation, large degradation of images was found in the far field. A computer simulation of the guided wave propagation reveals that a major reason for the degradation is the difference between dispersion curves for an actual pipe and the theoretical dispersion curves. In order to reduce the degradation, images were obtained by neglecting higher modes with larger differences in phase velocity. As a result, images were obtained at correct locations at distances of up to approximately 20 meters from the transducers.

Key words: Ultrasonic nondestructive inspection, Guided waves, Imaging, Long-range inspection

1. Introduction

When a low-frequency ultrasonic signal ranging approximately from 20 kHz to 200 kHz is input to a pipe, ultrasonic wave packets propagate in the longitudinal direction. The ultrasonic modes, called guided waves, can propagate up to a hundred meters in a pipe if they are appropriately excited. Recently, a long-range screening technique has been developed using such prominent characteristics of guided waves.

In the pipe inspection technique with guided waves, guided waves are generated from transducers and detected reflected waves from reflective objects, such as defects and weld lines, and can then be located based on arrival time of the reflected waves and the guided wave velocities. For easy analysis of the guided wave signals, non-dispersive axisymmetric modes are generated and received. However, information of the circumferential direction such as the circumferential location and width of defects cannot be obtained from the axisymmetric modes. Therefore, in the existing guided wave inspection tools, we cannot recognize from the echoes whether they indicate one defect, several defects, localized reflective objects, such as drill holes, or broad reflective objects, such as weld lines.

Therefore, the authors developed a technique for imaging reflective objects such as defects and weld lines using non-axisymmetric modes as well as axisymmetric modes [(1)],

*Received XX Xxx, 200X (No. XX-XXXX)
[DOI: 00.0000/ABCDE.2006.000000]

whereby many transducers arranged in the circumferential direction receive signals, which are then processed to obtain an image of the reflective objects. Figure 1 is a defect image for a pipe of 110 mm in diameter and 3.5 mm in thickness having two drill holes of 10 mm in diameter. In the figure, dark spots are located 1.2 m from the receiving transducers at 0° and 90°, which agrees well with the actual drill holes in the pipe. Thus, defects were able to be shown visually using reflective guided waves. However, a number of problems must be solved in order to enable practical application. For example, the image does not reveal whether an image that appears to contain a defect indicates a thru-hole or a broad defect, such as SCC, and this imaging technique has not been verified for large-range inspection.

The present study investigates the application of the imaging technique, which was verified only in the short range as Fig. 1, to long-range inspection though experiments using multiple reflections at both ends of a four-meter pipe and computer simulations for guided wave propagation.

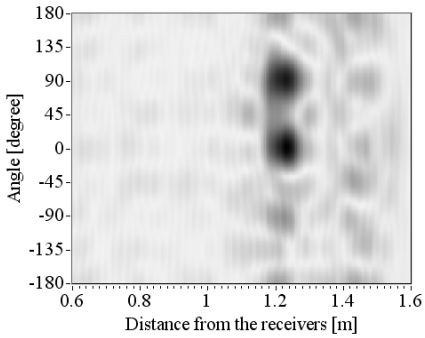

Fig. 1 Example of a defect image

2. Outline of defect imaging technique

The imaging technique using guided waves is outlined in this section. A detailed description is available in Reference (1). First, an inspection instrument consisting of transducers for exciting the axisymmetric torsional mode (T(0,1) mode) and transducers for receiving local circumferential vibrations are installed on an inspection pipe, as shown in Fig. 2. In Reference (1), magnetostrictive sensors and electromagnetoacoustic transducers (EMAT) were used to excite an axisymmetric mode and to receive local circumferential vibrations, respectively. On an aluminum pipe of 4 m in length, 110 mm in diameter, and 3.5 mm in thickness, two 10-mm-diameter thru-holes were drilled at 0º and 90º at 0.5 m from one pipe end, and an excitation magnetostrictive sensor and a receiving EMAT were positioned 1.0 m and 1.2 m from the artificial defects. Guided waves were measured at eight different circumferential positions at every 45º, and the results described below were obtained from the eight signals.

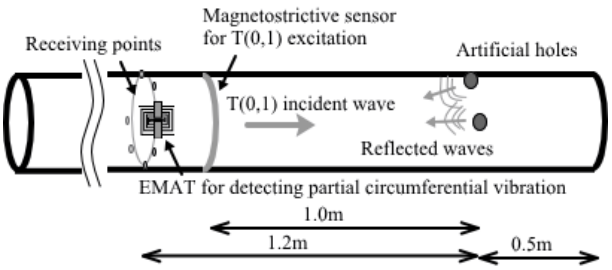

Fig.2 Locations of incident and receiving transducers and defects on a test pipe for a defect image in Fig.1.

The eight signals can be separated into waveforms for a certain guided wave mode by

summation using an appropriate weight [2]. The guided wave modes have different phase and group velocities that vary in frequency. These velocities are generally expressed in graphs of frequency versus velocity, called a dispersion curve, and are obtained by the analytical solution or calculation of the eigenvalue problem. Calculating the extracted waveforms with the theoretical dispersion curves gives the spatial waveforms at any time step.

Spatial waveforms, which were obtained by extracted modal signals from the reflected signals and were calculated with theoretical dispersion curves, are shown for each mode at 318 μs in Fig. 3. The time at which the incident T(0,1) mode arrives at the artificial defects is 318 μs, which is obtained by the distance between the excitation sensor and the artificial defect (1.0 m) divided by the velocity of the T(0,1) mode (3,120 m/s). The horizontal and vertical axes denote the distance from the receiving EMAT and the circumferential angle, respectively. The light and shaded area illustrate the amplitude of the waveforms. In the figure, n denotes the mode for the nth family, and each figure shows the spatial waveform for a T(n,1) mode(2). The figure for n=0, i.e., axisymmetric modes with constant phase in the circumferential direction, shows straight striped patterns, while the figure for n=1, i.e., a wave structure of $\sin\theta$, has two nodes in the circumferential direction. As n increases, the guided wave modes develop increasingly complex wave structures with $\sin n\theta$ in the circumferential direction [3]. In the imaging technique, $\exp(in\theta)$ is used instead of $\sin n\theta$, in order to consider the positive and negative rotations in the circumferential direction. The figures for n=1, 2, 3, and 4 in Fig. 3 show the sum of +θ and –θ rotation modes ($\exp(in\theta)$ and $\exp(-in\theta)$).

Summing these estimated spatial waveforms for each mode gives the spatial waveforms at this moment, as shown in the right lower image of Fig. 3. Such estimated spatial waveforms are obtained for every time step, and the propagation of reflected waves from defects can be seen, as shown in Fig. 4. At the moment when the incident wave just arrives at the defects, a large reflection can be seen at the defects. Since the areas where the incident wave arrives at each moment (dashed squares in Fig. 4) are known, summing these areas for every time step yields a single defect image. Figure 1 shows the summation of the incident wave areas for every time steps, as in the bottom-right panel in Fig. 4.

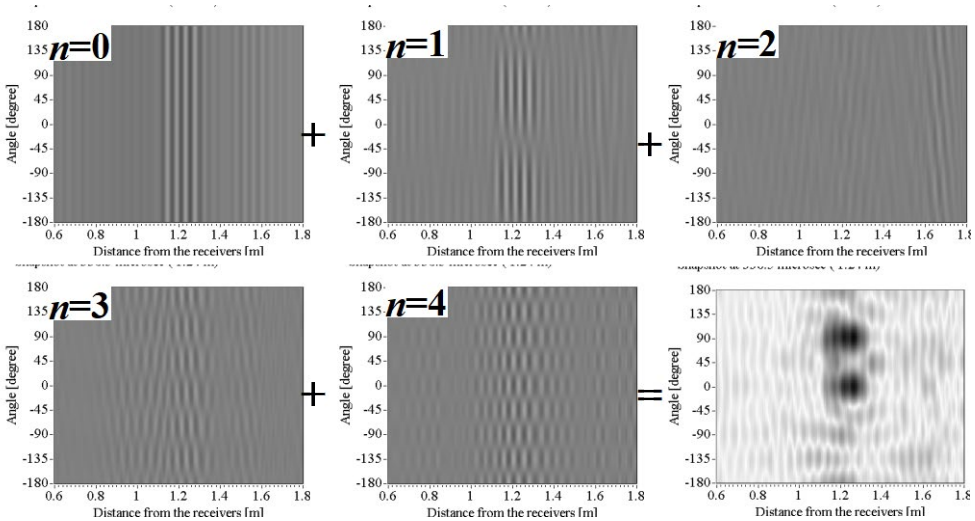

Fig.3 Spatial waveforms for each family and their summation at the moment when an incident wave arrives at the defects.

From the detected signals, we can estimate the longitudinal distance between the transducers and defects using group velocity, but we cannot recognize the existence of two artificial defects. In contrast, we can easily recognize two defects located at 0° and 90° at a

distance of 1.2 m from the transducers in the image. Since the image is obtained from the spatial waveforms, the minimum size of the defect image depends on the product of the wavelength and the number of cycles of the incident wave in the longitudinal direction, and the mode order in the circumferential direction. Therefore, considering the incident wave and the detected maximum mode order in this experiment, the minimum size of the defect image in the longitudinal direction is estimated to be approximately 176 mm (= wavelength 44 mm × four cycles) for the incident wave with a center frequency of 70 kHz, and that in the circumferential direction is estimated to be approximately 72º from 360º/5. In the experiment, the detected maximum mode order was four and the quantity 5 is the mode order plus one. Thus, the size of defect cannot be represented in the image.

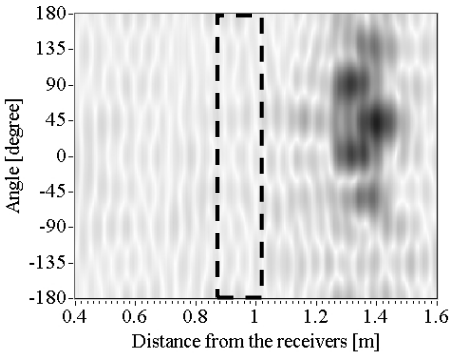

(a) t = 292 μs, before the incident wave arrives at the defects.

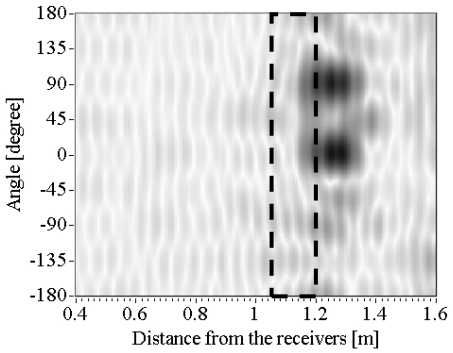

(b) t = 327 μs, the moment at which the incident wave arrives at the defects.

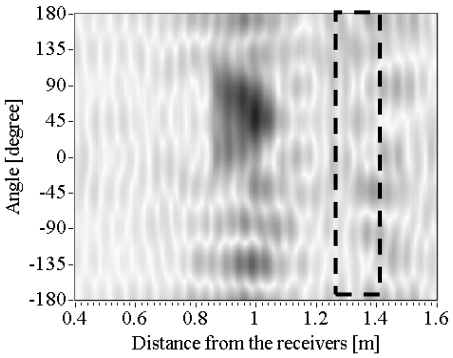

(c) t = 422 μs, after the incident wave passes the defects.

Fig.4 Spatial waveforms at three different time steps.
The dashed-line boxes indicate summed incident wave regions

and result in one defect image.

In the guided wave theory with no ultrasonic attenuation, as the frequency increases, the resolution in the longitudinal and circumferential directions becomes higher because the wavelength becomes shorter, and modes with a higher circumferential order can propagate. For example, for the same pipe used in the previous experiment, when 200 kHz is used as the input frequency, the wavelength of a T(0,1) mode is 1.55 mm, and the maximum circumferential order is approximately n=20. That is, the resolution becomes approximately the order of the wavelength (a few mm) in the longitudinal direction and approximately 16 mm ((diameter 110 mm × π)/(20+1)) in the circumferential direction.

Actually, as the frequency increases, it becomes more difficult to measure ultrasonic signals after a long propagation due to higher attenuation. Therefore, in defect imaging using guided waves, the resolution of the image and the range of the imaging are in a trade-off relationship. Since one of the biggest motivations in the use of guided waves is fast long-range inspection for pipes, increasing the frequency for higher resolution in the defect images is not essential. Guided wave pipe inspection equipment uses a frequency range below approximately 200 kHz. In the frequency range, the imaging technique using guided waves gives an unclear defect image that indicates the longitudinal and circumferential positions and the approximate size. Therefore, inspection personnel estimate the degree of damage using an obscure defect image, as well as their experience accumulated at the inspecting site.

3. Imaging of an excitation source in long-range inspection of a pipe

To investigate the effect on the defect image of long-range inspection, multiple reflections between both ends of a 4-m aluminum pipe were used. The test pipe was 110 mm in diameter and 4.0 mm in thickness, and the phase and group velocity dispersion curves for torsional modes are shown in Fig. 5. An electromagnet acoustic transducer (EMAT) generates a shear horizontal wave having a center frequency of 80 kHz and a four cycle bust wave, which models reflected waves from a defect of the same size with the active region of approximately 10 mm x 10 mm. The signal level was approximately the same as the signals of the reflected waves from the defect used to obtain Fig. 1, which implies that the SH wave excited from the EMAT could follow the waves reflected from the defect. A magnetostrictive sensor that can receive local SH vibration was used as a receiving transducer. Figure 6 shows the positions of an excitation EMAT and a receiving magnetostrictive sensor on a test pipe. Considering the sensor location, the propagation paths of guided waves can be drawn as A – D in order of propagation distance. In addition to paths A – D, multiple reflected waves at both ends of the pipe are measured, and so the distances of the propagation path are 1.4+8N, 3.4+8N, 4.6+8N, and 6.6+8N (m), where N is the number of round trips. Source images were obtained using eight signals detected at eight circumferential positions of the receiving transducer 1.6 m from the left end.

Figure 7 shows the waveform detected at one transducer position, and Fig. 8 shows a source image from 0 m to 16 m obtained by such detected signals. The arrows in Fig. 8 denote the source locations for propagation paths A – D and one round trip of these paths. Figure 9 shows an averaged waveform of the eight measured signals. The horizontal axis shows the propagation distance of the mode as well as time. The averaged waveform represents the waveform of the axisymmetric mode that is generally used for pipe inspection with guided waves. The velocity of the axisymmetric mode is equal to the shear wave velocity of the material (3,120 m/s). Therefore, pulse peaks were obtained at approximately 1.4+8N, 3.4+8N, 4.6+8N, and 6.6+8N (m) in Fig. 9 even in the long range. On the other hand, the source images in Fig. 8 were obtained clearly only for the first four

source images at 0º and accurate longitudinal positions, but in a long range exceeding 8 m, the source images appear unclear and occupy different positions. Note that the source size is not shown even in the first four dark areas because the wavelength used was approximately 38.5 mm.

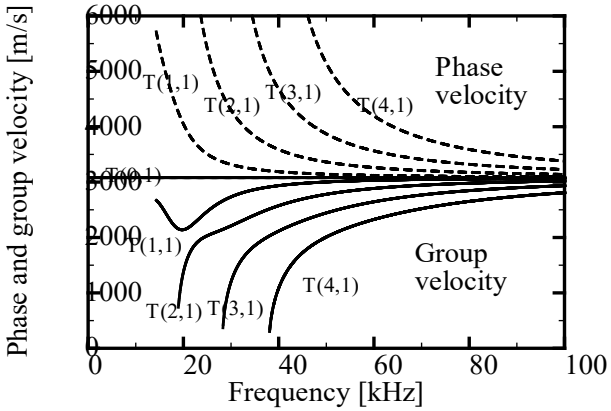

Fig.5 Phase and group velocity for a test pipe.

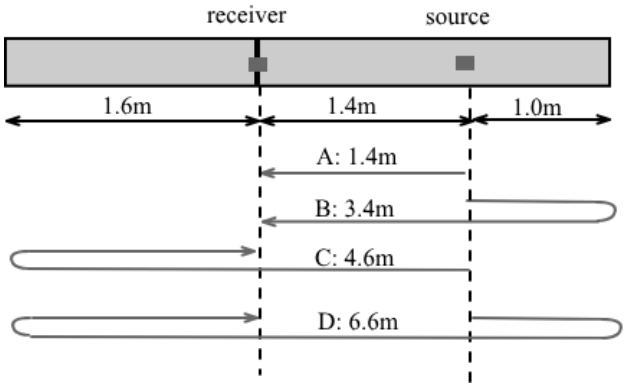

Fig.6 Sensor locations in a pipe and paths of guided wave propagation. **[In this figure, please insert a space between the number and unit.]**

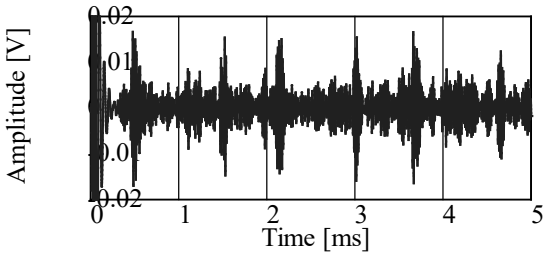

Fig. 7 Received signals at the first point.

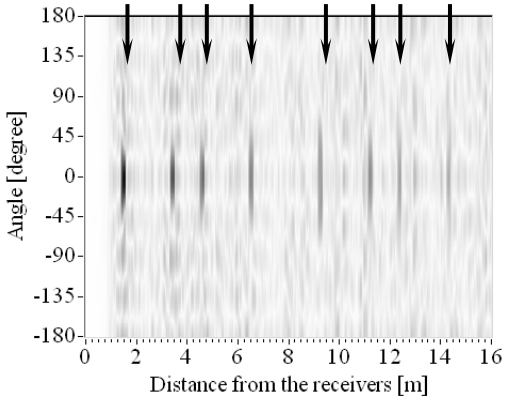

Fig. 8 Image of source locations.

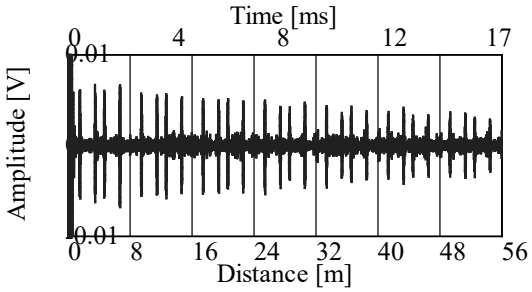

Fig. 9 Waveform of the axisymmetric T(0,1) mode.

4. Discussions on degradation of the images

Degradation of source images was observed beyond approximately 10 m in Fig. 8, in which expected source areas sometimes became lighter or darker. On the other hand, guided wave signals were confirmed even over propagation distances of 50 m in the waveform of the axisymmetric mode, as shown in Fig. 9. That is, guided wave signals could be detected, but degradation of the images occurred due to inappropriate processing of the signals. The authors described the effect of mismatches between several transducers around a pipe on defect images in a previous paper[1], where image degradation was observed when a time shift of approximately one half period was given to a signal detected at a certain transducer. In the case of Fig. 8, however, since source images were obtained in the near regions, the image degradation was not caused by errors between the transducers.

In order to investigate the cause of the degradation, Fig. 10 shows the spatial waveforms for each mode constructed before the source image of Fig. 8. Figure 10(a) shows the spatial waveform of the axisymmetric mode obtained from extracted waveforms for n=0, and Figs. 10(b), (c), (d), and (e) show the spatial waveforms of the axisymmetric mode obtained from extracted waveforms for non-axisymmetric modes n=1, 2, 3, and 4, respectively. Similar to Fig. 3, darker shades indicate higher amplitude. The spatial waveform of the axisymmetric mode n=0, shown in Fig. 10(a), was obtained by giving a constant distribution function in the circumferential direction to waveform of the axisymmetric mode, which was obtained by summing all eight signals. In Figs. 10(a) and (b), dark lines are located on the source position, but higher order modes, such as those shown in Figs. 10(c), (d), and (e) and longer distances have more differences. In particular, in Figs. 10(d) and (e) in the range over 5 m, distinct dark lines cannot be seen at the arrows indicating where the sources are located. The final source image, which is obtained by summing these spatial waveforms, would give errors due to differences in the higher modes. The source images were obtained with theoretical dispersion curves that can be derived from material properties and pipe geometry. Therefore, the degradation of images was caused by the difference between theoretical and actual dispersion curves for the pipe used. Figure 1 also shows slightly dark areas at locations other than the defect locations of 0º and 90º, which could also be caused by the difference between theoretical and actual dispersion curves.

In order to verify the degree of image degradation caused by the difference in the theoretical dispersion curves, guided wave propagation was calculated with Pipe Wave [4], a software package developed by our group. A guided wave with a center frequency of 80 kHz was emitted at 0° and detected 10 m away at eight circumferential positions in the computer simulation. When using the signals calculated by the simulation and theoretical dispersion curves, we can obtain an ideal image with no differences in theoretical dispersion curves, as shown in Fig. 11, in which a dark area appears at 10 m and 0º. Next, the difference in diameter of a pipe is considered to result in differences in the dispersion

curves. Usually, commercially available pipes have small differences in diameter, thickness, and material properties among companies. The test pipes used in the present experiments have a nominal thickness of 3 mm and a nominal diameter of 110 mm, although the actual dimensions of the pipes varied from 110 mm to 111 mm in diameter and 3.5 mm to 4.0 mm in thickness. Therefore, the source image was obtained using the dispersion curves for a 111-mm pipe, which is 1 mm larger than the pipe used in the numerical calculation of guided wave propagation. Figure 12 is the source image in this case. Compared to the ideal source image of Fig. 11, the dark area in Fig. 12 stretches in circumferential direction, which indicates degradation of the image. Figure 13 shows the dispersion curves for the pipes, where the solid lines and dashed lines denote the dispersion curves for a 110-mm pipe and a 111-mm pipe, respectively. Zoomed figures around the center frequency are shown in the insets for T(1,1) and T(2,1) modes, indicating that higher modes have more differences in phase velocity.

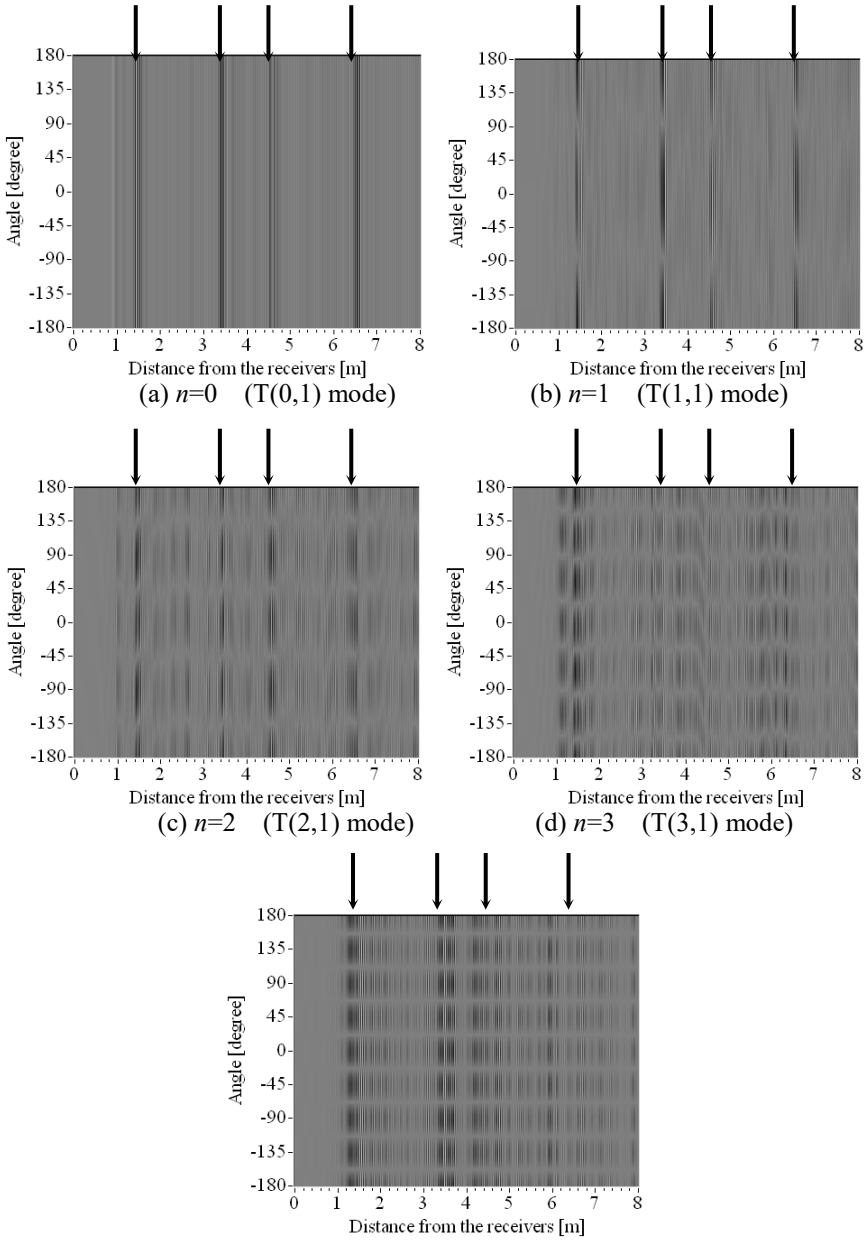

(a) n=0 (T(0,1) mode) (b) n=1 (T(1,1) mode)

(c) n=2 (T(2,1) mode) (d) n=3 (T(3,1) mode)

(e) n=4 (T(4,1) mode)

Fig.10 Images of source locations for each mode.

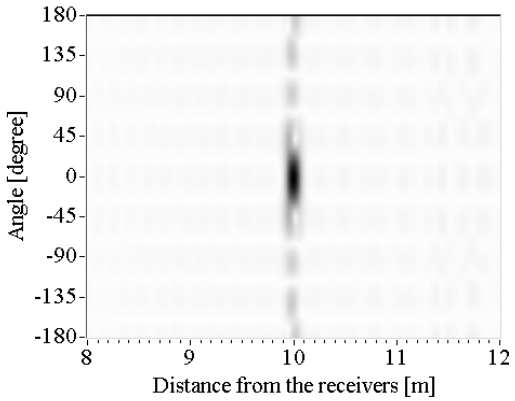

Fig.11 Ideal image of an excitation region using simulation data with Pipe Wave.

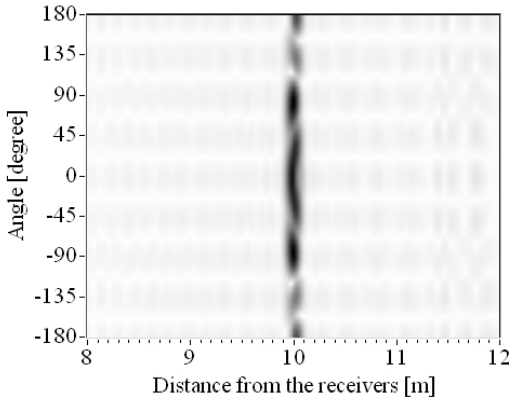

Fig.12 Image of an excitation region when the dispersion curve data has small differences.
Dispersion curves for a pipe having a diameter of 111 mm,
which is one millimeter larger than the original diameter, are used for imaging.

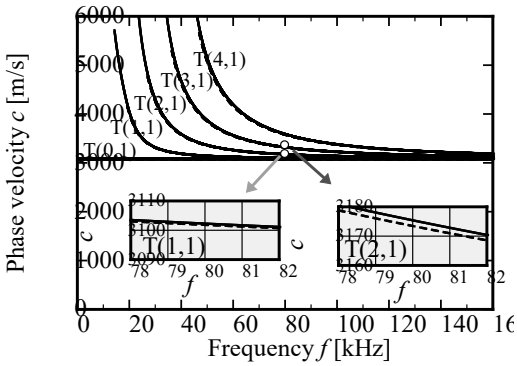

Fig.13 Torsional mode dispersion curves
for an aluminum pipe with 110 mm and 111 mm diameters.

5. Improvement of the imaging technique for long distances without high-order modes

Images close to the ideal image shown in Fig. 12 could be obtained by deriving accurate dispersion curves without any differences from the curves for an actual pipe. However, considering our previous studies on the experimental derivation of dispersion curves [5]-[7], it is expected that accurate derivation of dispersion curves within a few m/s is very difficult. Moreover, the differences between theoretical dispersion curves and the

dispersion curves for an actual pipe are caused by anisotropy of a pipe which is applied in a pultrusion process, as well as the differences in diameter and thickness. It is not practical to measure the anisotropy of a pipe for accurate derivation of a dispersion curve.

Thus, we conducted the imaging technique by neglecting high-order modes that have larger differences in phase velocity dispersion curves and considering the first two modes T(0,1) and T(1,1) to improve the degradation. Figures 14 and 15 show source images with low-order modes, in the regions from 0 m to 16 m and from 16 m to 32 m, respectively. Similar to Fig. 7, sources are located at the longitudinal location indicated by the arrows at 0º.

By comparison with the source image obtained in Fig. 7, the location of the source can be clearly identified even at a distance of approximately 14 m. In addition, in the more distant region shown in Fig. 15, source images can be obtained at the indicated locations at up to approximately 20 m and become unclear or show several lines at the indicated locations at over 20 m. This degradation of the image is caused by large phase differences in the long propagation distance.

On the other hand, dark regions in the circumferential direction in Fig. 14 become much longer than the actual source size and the dark regions in Fig. 7. This is because only T(0,1) and T(1,1) modes were used in Fig. 14, and T(0,1), T(1,1), T(2,1), and T(3,1) modes were used in Fig. 7. It can be concluded that circumferential size is expressed more accurately when using higher modes with a complex circumferential distribution.

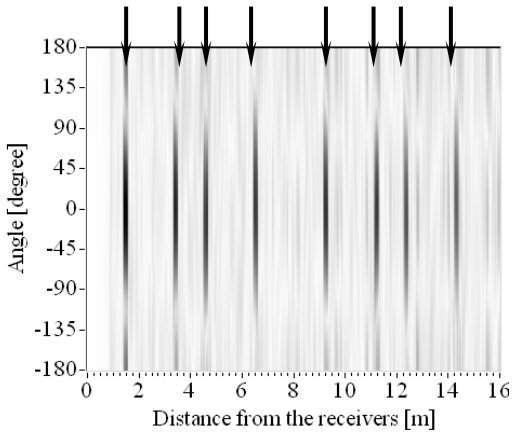

Fig.14 Image of excitation regions using lower modes, T(0,1) and T(1,1).

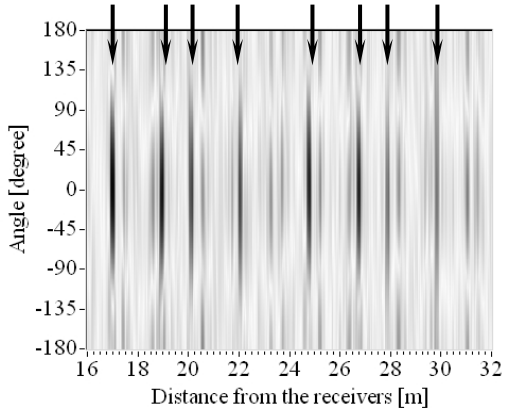

Fig.15 Image of excitation regions from 16 m to 32 m.

6. Conclusions

The present paper described the effect of long-range propagation of guided waves in an imaging technique that had been confirmed for a short propagation distance of a few meters. Many sources of guided waves at different locations appeared in the image using multiple

reflections between both ends of a 4-m pipe. In addition, numerical simulation of guided wave propagation was carried out in order to clarify the degradation of images over a long range. In a range of over approximately 10 m, the source images were degraded, even if the waveform of axisymmetric mode T(0,1) could be clearly obtained. It was demonstrated by numerical simulation of guided wave propagation that this degradation was caused by the differences between theoretical dispersion curves and the phase velocities of an actual pipe. Thus, an imaging technique using only low-order modes that have smaller differences in dispersion curves was proposed in the present study. Source images obtained using the proposed technique were located accurately in the longitudinal direction, even for a long range of approximately 20 m, but the locations were spread widely in the circumferential direction.

Since the diameter, thickness, and material properties of pipes are not given in most cases of actual inspection, the present improved imaging technique would be useful. We are considering whether more accurate images showing the characteristics of defects as well as their locations can be obtained by calibration of the dispersion curves by imaging known source locations.

References

(1) Hayashi, T. and Murase, M., *Journal of the Acoustical Society of America*, Vol. 117, No. 4 (2005) pp. 2134-2140
(2) Hayashi, T., et al., *Journal of the Japanese Society of Non-destructive Testing*, Vol. 53, No. 4 (2004) pp. 223-229
(3) Nishino, H., *Journal of the Japanese Society of Non-destructive Testing*, Vol. 52, No. 12 (2003) pp. 654-661
(4) Hayashi, T., et al., *Review of Progress in Quantitative Nondestructive Evaluation* Vol.25 (2006) pp. 173-180
(5) Alleyne, D. and Cawley, P., *Journal of the Acoustical Society of America*, Vol. 89, No. 3 (1991) pp. 1159–1168
(6) Nishino, H. et al., *Jpn. J. Appl. Phys*, Vol. 0, No. 1A (2001) pp. 364-370
(7) Hayashi, T. and Kawashima K., *JSME International Journal* (2003) pp. 620-62